# Adsorption of hexavalent chromium from aqueous solution by activated carbon prepared from almond shell: kinetics, equilibrium and thermodynamics study

M. K. Rai, B. S. Giri, Y. Nath, H. Bajaj, S. Soni, R. P. Singh, R. S. Singh and B. N. Rai

## ABSTRACT

Microporous activated carbon was prepared from almond shell powder and activated with $H_3PO_4$ and was used for the removal of Cr (VI). The characterization of activated carbon was done for Fourier transform infrared spectroscopy (FTIR), scanning electron microscopy (SEM), Brunauer–Emmett–Teller (BET) surface area measurement and elemental analysis. The batch experiments were conducted to study the effects of contact time, solution pH, adsorbent dose, initial chromium concentration and temperature on removal of Cr (VI). The Cr (VI) removal was found to be 100% at an initial pH of 2. The equilibrium data for the adsorption of Cr (VI) on the adsorbent were fitted with Langmuir, Freundlich, Temkin and Dubinin–Radushkevich adsorption isotherm models. The Langmuir isotherm model fitted better and values of model parameters $q_m$, $b$, $R^2$ and $R_L$ were found to be 195, 0.024, 0.98 and 0.45, respectively. Adsorption kinetics was analyzed for the pseudo first order, pseudo second order and intra-particle diffusion situations. Thermodynamic parameters revealed the spontaneous, endothermic and increased randomness nature of the adsorption process. The values of $\Delta H^\circ$ and $\Delta S^\circ$ were found to be 22.9 KJ/mol and 95.3 J/mol-K.

**Key words** | activated carbon, adsorption, almond shell hexavalent chromium, kinetics

**M. K. Rai**
**B. S. Giri** (corresponding author)
**Y. Nath**
**H. Bajaj**
**S. Soni**
**R. S. Singh**
**B. N. Rai**
Department of Chemical Engineering & Technology,
IIT (BHU),
Varanasi, 221005, U.P.,
India
E-mail: *balendushekher23@gmail.com*

**R. P. Singh**
Department of Municipal Engineering,
Southeast University,
Nanjing 210096,
China

## INTRODUCTION

Chromium is present in industrial effluents produced from electroplating, leather tanning, cement, mining, textile dyeing, dye manufacturing, paper, ink, aluminum conversion coating operations, steel fabrication, plants producing industrial inorganic chemicals, wood treatment units, paints and pigments, metal cleaning, fertilizer and photography industries and cause severe environmental and public health problems (Anupam *et al.* 2011; Tan *et al.* 2015). In general, industrial wastes contain both hexavalent and trivalent forms of chromium (Nakajima & Baba 2004; Sonwani *et al.* 2018). Cr (III) is nearly insoluble and hence aqueous concentrations are usually well below water quality standards (Anderson *et al.* 1994). The hexavalent species are relatively more soluble and are 500 times more toxic than the trivalent species (Gupta & Babu 2009). It is proven to cause skin irritation, epigastric pain, nausea, vomiting, severe diarrhea, hemorrhage and carcinogenicity in humans (Mohanty *et al.* 2005; Wang *et al.* 2014). According to the World Health Organization (WHO), the permissible level in surface water bodies should be lower than 0.05 mg/L. Therefore, it is necessary to reduce Cr (VI) to acceptable levels before discharging effluents into aquatic environments.

Conventional technologies for Cr (VI) removal from aqueous solutions include chemical reduction/precipitation, ion-exchange, membrane separation, and adsorption (Imai

doi: 10.2166/aqua.2018.047

& Gloyna 1990; Selvi *et al.* 2001; Stasinakis *et al.* 2003; Owlad *et al.* 2009; Sonwani *et al.* 2018). Increasing attention has been paid recently to the use of eco-friendly and low-cost biomaterials as adsorbents/bio-sorption for Cr removal from wastewater, such as bacteria, fungi, algae, industrial and agricultural wastes (Mohan *et al.* 2006; Han *et al.* 2007; Park *et al.* 2007; Singh *et al.* 2017). Most of these methods suffer various drawbacks such as from high operational costs, unreliable nature of operation, etc. Adsorption is a reliable and cost effective method provided that the adsorbent used in the process has good adsorption capacity and is cheaply available. Many studies have been done on adsorptive removal of Cr (VI) from waste by using activated carbons derived from different materials (Table 1). However, there is very limited published information available on the use of almond shell for preparation of activated carbon and its application for the removal of Cr (VI).

Almond is a dry fruit which is produced in several countries including India. The shell of almond fruit is a very good agro-waste and excellent adsorbent. Since it is primarily lingo-cellulosic in nature and hard, it can be used as a feed-stock for making activated carbon for adsorption of water pollutants including Cr (VI) to save the woody biomass which is used for preparation of activated carbon at industrial scale. Keeping this view, almond shell was used as a raw material to produce biochar which was finally activated using $H_3PO_4$. The prepared activated carbon was used for removal of Cr (VI) in batch adsorption experiments under optimum operating conditions.

## MATERIALS AND METHODS

### Adsorbate: chromium (VI)

All the solutions were prepared by using deionized water, and stock solution of 1,000 mg/L Cr (VI) was prepared by dissolving potassium dichromate (analytical reagent [AR] grade). The test solutions of Cr (VI) were prepared by diluting the stock solutions to specific concentrations as per the requirements.

### Preparation of activated carbon

The almond shells were obtained from the local market. The shells were crushed in the disintegrator and sieved to obtain 14–72 mesh (BSS, British Standard Sieve) fractions. Chemical activation of the powdered shells was performed with 40% $H_3PO_4$ (AR grade) using the procedure reported by Girgis *et al.* (2002). The impregnation ratio of 3:1 (weight of $H_3PO_4$:weight of powdered shells, w/w) was used for

**Table 1** | Comparing of different activated carbon as Cr (VI) adsorbent

| Activated carbon sources | Initial pH | BET surface area ($m^2\ g^{-1}$) | Pore volume ($cm^3\ g^{-1}$) | Maximum adsorption capacity ($mg\ g^{-1}$) | References |
|---|---|---|---|---|---|
| Tamarind wood | 2 | 1,322 | 1.042 | 28 | Acharya *et al.* (2009) |
| Apricot stone | 2 | 1,462 | 0.6338 | 262 | Ozdemir *et al.* (2011) |
| Rubber wood sawdust | 2 | 1,673 | – | 65 | Karthikeyan *et al.* (2005) |
| Coconut shell fibers | 2 | 1,565 | 0.65 | 21.75 | Mohan *et al.* (2005) |
| Terminallia Arjuna nuts | 1 | 1,260 | – | 28.43 | Mohanty *et al.* (2005) |
| Bael fruit | 2 | – | – | 17.27 | Kumar & Mandal (2009) |
| Peanut shell | 2 | 95.51 | 0.35 | 16.26 | Othman *et al.* (2012) |
| Longan seed | 3 | 1,511.8 | 0.742 | 35.02 | Yang & Chen (2015) |
| *Sterculia guttata* shell | 2 | 498.29 | 0.232 | 45.5 | Rangabhashiyam & Selvaraju (2015) |
| Sal sawdust | 3.5 | – | – | 9.55 | Baral *et al.* (2006) |
| Almond shell | 2 | 1,223 | 0.326 | 167.5 | Present study |

proper penetration and the mixture was kept for 24 h. The chemically mixed sample was dried in the oven at 70 °C for 10 h. The dried pre-treated almond shell powder was carbonized at 600 °C for 2 hours in a laboratory muffle furnace (NSW India, NSW-101). The cooled carbonized sample was washed thoroughly with distilled water and its pH was adjusted to 7 with 1N HCl and 1N NaOH. The sample was then dried at 70 °C overnight. The carbonized almond shell activated carbon (ASAC) then obtained was kept in airtight bottles for characterization and adsorption experiments.

## Physicochemical characterization of activated carbon

The physicochemical characterizations of the samples were carried out in order to know their chemical composition, functional groups, morphology, and surface area. Various functional groups present on the surface of activated carbon were analyzed using a Fourier transform infrared spectroscopy (FTIR) analyzer (Scientific, Nicolet 5700).

The surface morphology was analyzed using scanning electron microscopy (SEM) (FEI™, Quanta 200F) to determine the surface texture and the porosity. The average pore size or diameter was also calculated using SEM results.

The elemental analysis of the almond shell powder and activated carbon were determined by using an elemental analyzer (Euro-EA) and results are presented in Table 2. The surface area, pore volume and pore size of the almond shell powder and activated carbon were determined using the $N_2$ adsorption at −196 °C and $N_2$ desorption at ambient temperature with degassing at 300 °C using a Smart Sorbs 92/93 surface area analyzer (Smart Instruments Co. Pvt. Ltd).

**Table 2** | Physical properties of almond shell activated carbon

| Parameters | Value |
|---|---|
| BET surface area ($m^2\ g^{-1}$) | 1,223 |
| Pore volume ($cm^3\ g^{-1}$) | 0.326563 |
| Average pore size (nm) | 2.39 |
| pH at the point of zero surface charge ($pH_{pzc}$) | 5.5 |
| Elemental analysis (%) | |
| C | 75.56 |
| H | 2.55 |
| N | 1.45 |
| S | 0 |
| O | 15.44 |

The pH value required to give zero net surface charge is $pH_{pzc}$. The surface is positively charged below this pH and negatively charged above this pH. A plot of the equilibrium pH versus initial pH yielded a curve from where the $pH_{pzc}$ was identified as the point at which the change of pH is zero.

## Adsorption experiments

The adsorption experiments were conducted in 250 mL Erlenmeyer flasks containing 100 mL solution of Cr (VI) to investigate the effects of contact time (0–300 min), solution pH (2–10), adsorbate dose (0.25–1.0 g/100 mL), initial concentration (50–1,000 mg/L) and temperature and obtain their optimum values. All adsorption experiments were carried out at a constant agitation speed of 150 rpm.

Equilibrium adsorption data were obtained by conducting the experiments at various temperatures (298, 303, and 308 K), with sample solutions containing varying concentrations of Cr (VI) ranging from 50–1,000 mg/L. An adsorption kinetic study was performed by adding a dose of 0.25 g/100 mL at pH 2 with varying Cr (VI) concentrations of 100, 150, 250 and 300 mg/L at 308 K and analyzing the samples after consistent intervals of time.

The applicability of different absorption isotherm models was studied using the experimental findings. The residual concentration of adsorbate was determined by measuring the absorbance of the purple complex of Cr (VI) with 1,5–diphenyl carbazide at 540 nm using a UV-spectrophotometer (Elico, SL 159). The difference in Cr (VI) concentration before and after the adsorption was used to calculate the percentage adsorption of Cr (VI). The amount of adsorbed Cr (VI) per gram of activated carbon was calculated using Equation (1):

$$q_e = \frac{(C_0 - C_e)V}{W} \quad (1)$$

where $C_0$ (mg/L) and $C_e$ (mg/L) are the initial and equilibrium concentration of Cr (VI) respectively, $V$ (L) is the

volume of solution, $W$ (g) is the mass of activated carbon, and $q_e$ (mg/g) is the metal uptake capacity of activated carbon.

## Adsorption isotherms

Adsorption isotherms provide useful information, including the adsorption mechanism for the adsorption of Cr (VI) on the adsorbent surface, and are also important in the designing of adsorption systems. The two parameter isotherm models like Langmuir, Freundlich, Temkin and Dubinin–Radushkevich (D–R) were used to analyze the equilibrium data obtained in the present study.

## Langmuir isotherm

The Langmuir isotherm model (Langmuir 1918) is valid for the monolayer adsorption which assumes that all active sites of adsorption are homogeneous in nature and the adsorption at one site does not affect an adjacent active site of adsorption. The linear from of the Langmuir isotherm model is expressed by Equation (2):

$$\frac{C_e}{q_e} = \frac{C_e}{q_m} + \frac{1}{bq_m} \tag{2}$$

where $b$ is the adsorption equilibrium constant (L/mg) related to the energy of adsorption and $q_m$ (mg/g) is the quantity of adsorbate required to make a single layer on a unit mass of adsorbent.

A further analysis of the Langmuir isotherm can be made on the basis of a dimensionless equilibrium parameter, $R_L$, also known as the separation factor and given by Equation (3):

$$R_L = \frac{1}{1 + bC_0} \tag{3}$$

where $b$ is the adsorption equilibrium constant (L/mg) related to the energy of adsorption and $q_m$ (mg/g) is the quantity of adsorbate required to make a single layer on a unit mass of adsorbent. The value of $R_L$ lies between 0 and 1 for a favorable adsorption, while $R_L > 1$ represents an unfavorable adsorption, and $R_L = 1$ represents linear adsorption, while the adsorption operation is irreversible if $R_L = 0$.

## Freundlich isotherm

The Freundlich model is an empirical equation which assumes that the active sites of adsorption are heterogeneous in nature and adsorption at one site affects the adsorption at the adjacent site. Kanjanarong *et al.* (2017) reported the linearized form of the Freundlich isotherm model. The linearized form of the Freundlich isotherm model can be expressed as in Equation (4):

$$\ln q_e = \ln k_f + \frac{1}{n} \ln C_e \tag{4}$$

where $K_f$ and $n$ are the Freundlich isotherm constants. $K_f$ (mg/g (L/mg)$^{1/n}$) indicates the adsorption capacity and $n$ stands for the intensity of the adsorption.

## Temkin isotherm

The Temkin isotherm model contains a factor that describes the interactions between adsorbent and adsorbate (Tempkin & Pyzhev 1940; Dada *et al.* 2012). This model assumes that the heat of adsorption of all the molecules in the layer decreases linearly due to the coverage of adsorbate molecules, and the adsorption of adsorbate is uniformly distributed. This model also assumes that the decrement in the heat of adsorption is linear rather than logarithmic, as used in the Freundlich isotherm model. The non-linear form of the Temkin model is given by Equation (5):

$$q_e = \frac{RT}{b_t} \ln (A_T C_e) \tag{5}$$

The above equation can be simplified as given by Equation (6):

$$q_e = B_T \ln A_T + B_T \ln C_e \tag{6}$$

where $B_T = (RT)/b_T$, $R$ is the universal gas constant (8.314 J mol/K) and $T$ (K) is the absolute temperature. The constant $b_T$ describes the heat of adsorption and $A_T$

explains the equilibrium binding constant (L/min) corresponding to maximum binding energy. A graph of $q_e$ versus ln $C_e$ is used to calculate the Temkin isotherm constants, $A_T$ and $b_T$.

### Dubinin–Radushkevich isotherm

The D–R isotherm model is used to estimate the nature of the adsorption process, whether it is physical or chemical (Dubinin & Radushkevich 1947; Dada *et al.* 2012). The D–R isotherm is more general than the Langmuir isotherm because this model is not based on the assumption of a homogeneous surface or constant adsorption potential, but the apparent energy of adsorption is calculated. The D–R model is represented using the following non-linear Equation (7):

$$q_e = q_m \ \exp(-K\,\varepsilon^2) \tag{7}$$

where $K$ is a constant related to adsorption energy (mol$^2$/J$^2$). $\varepsilon$, the Polanyi potential is calculated from the equation, $RT$ ln (1+ (1/$Ce$)), where $R$ (J/mol K) is the universal gas constant and $T$ is the temperature. The mean free energy of adsorption ($E$) is calculated using Equation (8):

$$E = \frac{1}{\sqrt{2K}} \tag{8}$$

The $E$ value gives information about the adsorption type; if the value of $E < 8$ kJ/mol the adsorption process is governed by physisorption, while for $E > 16$ kJ/mol chemisorption prevails.

### Kinetic studies

In order to analyze the kinetics of the adsorption process, the equilibrium data were fitted to pseudo-first-order, pseudo-second-order and intra-particle diffusion models. To investigate the adsorption kinetic, experiments were performed at different initial concentrations of Cr (VI) at pH 2, temperature of 35 °C and dose of 2.5 g/L. The contact time was set to 240 min in each experiment to ensure each adsorption process could reach the equilibrium value.

### Pseudo first and second order models

Lagergren proposed a model on pseudo-first-order kinetics (Kanjanarong *et al.* 2017). The linearized-integral form of the pseudo-first-order model is represented as Equation (9):

$$ln(q_e - q_t) = ln\, q_e - k_1 t \tag{9}$$

where $q_e$ and $q_t$ are the sorption capacities at equilibrium and at time $t$ (mg/g), respectively, and $k_1$ is the rate constant of pseudo-first-order sorption (min$^{-1}$). The values of $k_1$ and $q_e$ can be determined from the slope and intercept of the graph of $ln\ (q_e{-}q_t)$ versus $t$.

The pseudo-second-order sorption kinetics (Kanjanarong *et al.* 2017) can be expressed as shown in Equation (10):

$$\frac{t}{q_t} = \frac{1}{k_2 q_e^2} + \frac{t}{q_e} \tag{10}$$

where $q_e$ and $q_t$ are the sorption capacity at equilibrium and at time $t$ (mg/g), respectively, and $k_2$ is the rate constant of the pseudo-second-order sorption (g/mg-min) which can be determined by plotting the graph of $t/q_t$ versus $t$.

### Intra-particle diffusion model

The intra-particle diffusion model was proposed by Weber and Morris (Weber & Morris 1962) and describes information about mechanisms and rate controlling steps in the adsorption kinetics. This equation provides information about the rate-limiting step in the adsorption process. This may occur due to the diffusion of the adsorbate into the adsorbent layer. The model is represented using the following equation:

$$q_t = k_{id} t^{1/2} + I \tag{11}$$

where $k_{id}$ is the intra-particle diffusion rate constant (mg/g min$^{1/2}$), and the value of $I$ (mg/g) represents the thickness of the boundary layer. The values of $I$ and $k_{id}$ are obtained from the intercept and slope of the curve, respectively.

### Thermodynamic study

In order to find out the nature of the adsorption process, the mechanism, spontaneity and heat change in adsorption of

Cr (VI) on ASAC, it is important to determine relevant thermodynamic parameters. The enthalpy change, $\Delta H^{\circ}$, entropy change, $\Delta S^{\circ}$ and Gibbs free energy change, $\Delta G^{\circ}$, were determined using:

$$\Delta G^{\circ} = -RT \ln K_0 \tag{12}$$

$$\ln K_0 = \frac{\Delta S^{\circ}}{R} - \frac{\Delta H^{\circ}}{RT} \tag{13}$$

where $T$ is the absolute temperature (K), $R$ is the gas constant (8.314 J/mol K) and $K_0$ is the distribution coefficient calculated using the following equation:

$$K_0 = \frac{q_e}{c_e} \tag{14}$$

Thermodynamic properties were calculated by plotting the graph of $ln\ K_0$ versus $1/T$.

### Statistical analysis

Maximum experimental findings were analyzed by statistics software tools. These data were calculated and the values of average, standard deviation and relative standard errors (RSE) were found. For the other parts of the experiments, mostly single experiments were carried out in this work.

## RESULTS AND DISCUSSION

### Characterization of activated carbon

The $pH_{pzc}$ value of ASAC was found to be 5.5, which indicates that at this pH the net surface charge of the activated carbon is zero, whereas at pH <5.5, the adsorbent surface is positively charged and at pH >5.5, it is negatively charged.

FTIR spectra of the adsorbent before and after adsorption were recorded in the range of 400–4,000 $cm^{-1}$. The following wave numbers appeared in ASAC: 650 $cm^{-1}$ indicated the C–H vibration in aromatic compounds; the peak at 1,590 and 1,385 $cm^{-1}$ corresponded to COO– and >C=O– groups, 1,820–1,900 $cm^{-1}$ corresponded to the >C=O– stretch of saturated carboxylic acids and aliphatic esters (Droussi *et al.* 2009; Zhang *et al.* 2011; Chia *et al.* 2012; Singh *et al.* 2017; Talha *et al.* 2018). The peaks around 2,760.5–1,899.5 $cm^{-1}$ might be assigned to aldehydes, carbonyls, carboxylic acids and esters present on the surface (Pedroza *et al.* 2014; Kanjanarong *et al.* 2017; Talha *et al.* 2018). These functional groups have an affinity toward chromium ions. FTIR spectra of Cr (VI) loaded ASAC show the shifted peak locations and low transmittance intensity at 3,428, 2,934, 1,634 and 1,246 $cm^{-1}$ due to Cr (VI) adsorption (Figure 1).

Differences in SEM images were observed between surface topography of ASAC before and after adsorption. SEM photomicrographs before and after adsorption are shown in Figure 2. From Figure 2, it is clear that ASAC has a highly porous structure with greater homogeneity. The SEM photomicrograph after Cr (VI) adsorption shows that a layer is formed due to Cr (VI) adsorption on the surface of the activated carbon and some Cr (VI) has also filled the pores.

From Table 2, it is observed, as expected, that the percent carbon content in activated carbon (78.0%) is substantially higher than that of raw almond shell (44.4%). This is nearly comparable to other activated carbon reported for olive pits (64.4%) (Ugurlu & Karaoglu 2008), sugar beet bagasse (70–80%) (Onal *et al.* 2007) and hazelnut-husk (80.4%) (Karacetin *et al.* 2014). The Brunauer–Emmett–Teller (BET) surface area of the adsorbent was found to be 1,223.4 $m^2/g$ which indicates that ASAC may be a good

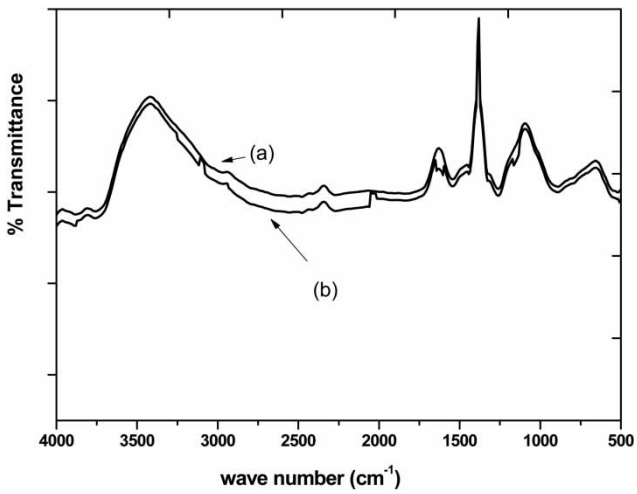


**Figure 1** | FTIR spectra of the almond shell activated carbon (a) before adsorption and (b) after adsorption.

adsorbent for adsorption of Cr (VI) and other pollutants from wastewater (Table 2). The other important physical properties like pore volume, average pore size and point of zero charge of prepared activated carbon were found to be 0.3266 $cm^3/g$, 2.39 nm and 5.20 (Table 2), respectively, which may play an important role in the adsorption.

## Effect of adsorbent dose and contact time

Adsorbent dose and contact time are important parameters for the adsorption, in the study of maximum Cr (VI) adsorption capacity. From Figure 3, it is observed that the removal of Cr (VI) is rapid in the early stages up to 100 minutes and becomes almost constant after 240 minutes. This may be due to the availability of more adsorption sites for the removal of Cr (VI) ions at the initial stage, and after some time the slow rate of Cr (VI) adsorption is due to hindrance or repulsion of absorbed Cr (VI) ions onto the adsorbent surface (Hsu *et al.* 2009). It is observed that the uptake of Cr (VI) increases as amount of the adsorbent dose decreases. From Figure 3, it is clear that the adsorption capacities decreased from 16 to 4 mg/g as the dosage was increased from 2.5 to 10 g/L. Figure 3 shows that increasing the adsorbent dose above the optimum value did not result in an increase in the Cr (VI) ion uptake. This can be explained by the overlapped and unsaturated sites of the adsorbent (Rai *et al.* 2016). The optimum bio-sorbent dosage of 2.5 g/L and contact time of 240 min were selected for further adsorption experiments. The value of SD and SD error were found to be 24.3 and 2.40 for removal efficiencies. These values agree with the reported values for various pollutants (Giri *et al.* 2012). Using statistical analysis the standard deviation for the $Q_e$ values were calculated and found to be 4.79, 3.16, 2.24 and 1.89 while relative standard error (RSE) values were 14.4, 14.4, 15.0 and 16.7 for the concentrations of 1, 0.75, 0.5 and 0.25 g/100 mL, respectively.

## Effect of pH

Figure 4 exhibits the influence of pH (2–8) on the adsorption process. As seen from Figure 4, the uptake of Cr (VI) from aqueous solution is dependent on the pH value, and the maximum adsorption capacity is found to be 20 mg/g at pH 2.0. Increasing the pH value from 2.0 to 8.0 results in decreasing Cr (VI) adsorption capacity. This could be explained by the fact that Cr (VI) exists in ionic form and the existence of these ions, such as $CrO_4^{2-}$, $HCrO_4^-$ or $Cr_2O_7^{2-}$, depend on the pH of the aqueous solution

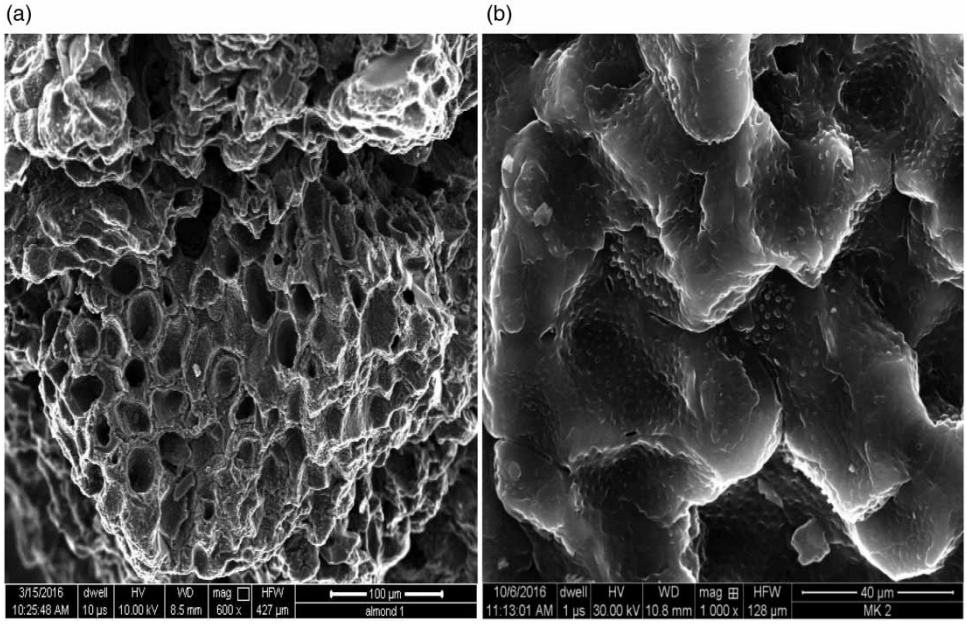


**Figure 2** | SEM micrographs of ASAC (a) before adsorption and (b) after adsorption of Cr (VI).

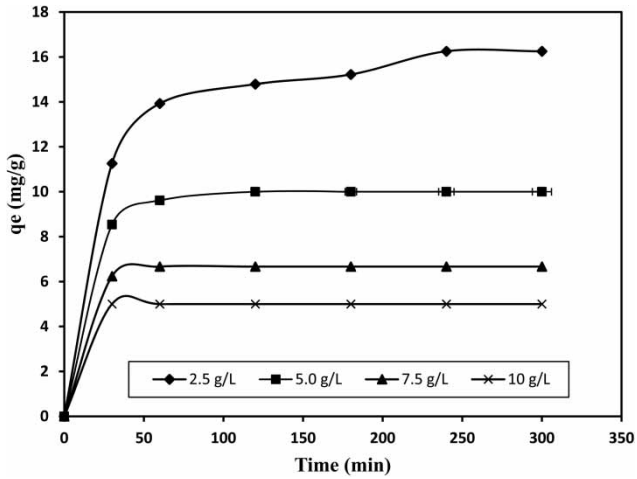


**Figure 3** | Effect of activated carbon dose and effect of time on metal uptake (initial con. 50 ppm, pH 6, agitation speed 150 rpm, pH 5.5, temperature 35 °C).

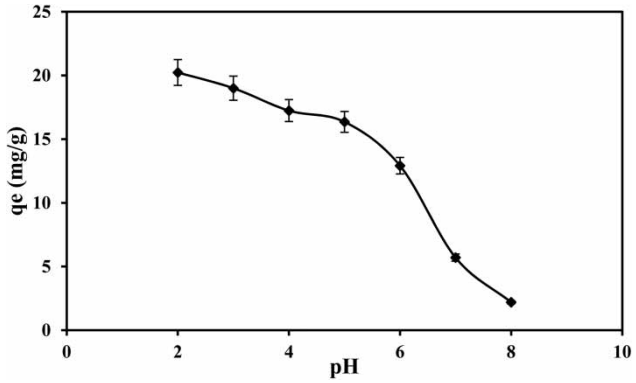


**Figure 4** | Effect of solution pH on metal uptake by almond shell activated carbon (initial concentration 50 mg/L, time 300 min, agitation speed 150 rpm, temperature 35 °C, dose 2.5 g/L).

(Suksabye & Thiravetyan 2012). Within the pH range of 2.0–6.0 $HCrO_4^-$ and $Cr_2O_7^{2-}$ ions are found in equilibrium, and after increasing the pH chromate ions ($CrO_4^{2-}$) predominate. $HCrO_4^-$ or $Cr_2O_7^{2-}$ ions need only one active site, whereas a chromate ion ($CrO_4^{2-}$) needs two active sites due to its two negative charges. Hence, an increase in the adsorption capacity of Cr (VI) is observed due to more $HCrO_4^-$ ions at lower pH values which need a single site for adsorption (Baral *et al.* 2006). At higher pH the adsorption capacity is decreased due to competitive adsorption between chromate and hydroxyl ions. The surface of the adsorbent was positively charged at a pH lower than the $pH_{pzc}$ and negatively charged at pH values greater than $pH_{pzc}$. Thus, the initial solution pH of 2.0 was selected as the optimum pH value for Cr (VI) adsorption for all the remaining experiments.

## Effect of initial Cr (VI) concentration

The effect of initial concentration on Cr (VI) removal by ASAC was studied at different initial Cr (VI) concentrations (100–1,000 mg/L) at a contact time of 240 min, pH of 2 and optimal adsorbent dosage of 2.50 g/L. The adsorption capacity increased from 40.0 to 168 mg/g as initial Cr (VI) concentration increased from 100 to 1,000 mg/L (Figure 5). Statistical analyses of findings were carried out using basic statistical software. Standard deviation was found to be 26.2 and relative standard error was 10.6 for removal efficiencies. The increase in adsorption capacity of the adsorbents with an increase in initial Cr (VI) concentration is due to more interaction of Cr (VI) ions with the absorbent surface (Verma *et al.* 2006; Nemr 2009). The percentage removal of Cr (VI) decreased from 100 to 40.5% with an increase in Cr (VI) concentration from 100 to 1,000 mg/L. The decrease in percentage removal of Cr (VI) is due to less active sites being available for Cr (VI) ions because their sites saturate above a certain concentration. Therefore, Cr (VI) removal was dependent on initial Cr (VI) concentration.

## Adsorption isotherm

The values of the isotherm parameter and the coefficient of determination ($R^2$) of four equilibrium models at different temperatures are shown in Table 3. The maximum adsorption capacities ($q_m$) determined by the Langmuir model were found to be 202.34, 197.34 and 195.34 mg/g at temperatures of 35, 30 and 25 °C, respectively. The coefficient of determination values ($R^2$) were found to be high for the Langmuir model in comparison to the other three models which confirmed the monolayer adsorption of Cr (VI) on ASAC. The calculated $R_L$ values were in the range 0–1 which indicated favorable adsorption of Cr (VI). Freundlich parameters were determined from the linear plot of ln ($q_e$) versus ln ($C_e$). The obtained $n$ values were greater than 1.0, which indicated a favorable Cr (VI) adsorption process. $R^2$ values for the Freundlich model were very low as compared to the Langmuir model, which suggests that

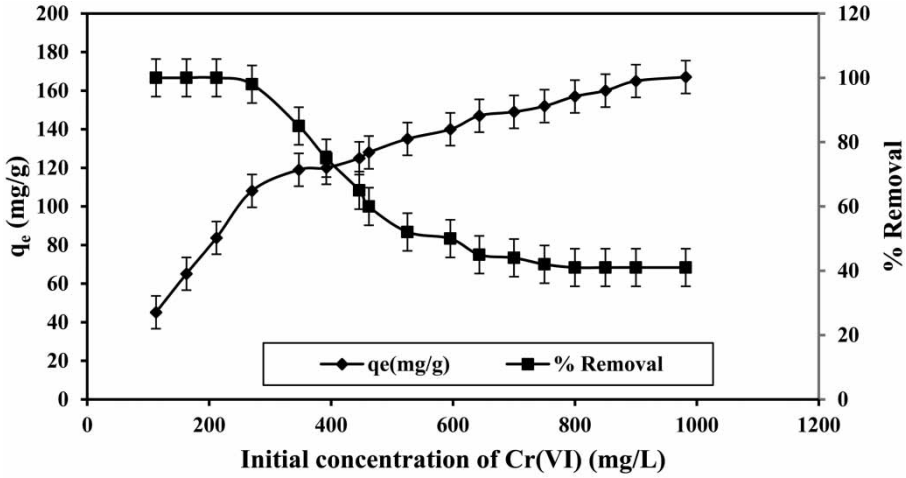


**Figure 5** | Effect of initial concentration of Cr (VI) on metal uptake and % removal by almond shell activated carbon (pH 2; time 4 h; agitation speed 150 rpm; temperature 35 °C; dose 2.5 g/L).

**Table 3** | Isotherm parameters for Cr (VI) adsorption on ASAC

| | | Temperature | | |
|---|---|---|---|---|
| **Adsorption isotherms** | **Parameters** | **25 °C** | **30 °C** | **35 °C** |
| Langmuir isotherm | $q_m$ | 195.34 | 197.34 | 202.34 |
| | $b$ | 0.024 | 0.027 | 0.018 |
| | $R^2$ | 0.976 | 0.964 | 0.986 |
| | $R_L$ | 0.4545 | 0.4255 | 0.5263 |
| Freundlich isotherm | $K_f$ | 79.35 | 80.74 | 84.34 |
| | $n$ | 1.334 | 1.247 | 1.124 |
| | $R^2$ | 0.8945 | 0.835 | 0.876 |
| Tempkin | $A_T$ | 862.64 | 701.345 | 627.63 |
| | $b_T$ | 226.67 | 223.32 | 220.18 |
| | $R^2$ | 0.643 | 0.661 | 0.712 |
| Dubinin–Radushkevich | $q_m$ | 132.55 | 133.54 | 134.42 |
| | $K \times 10^6$ | 3.02 | 2.50 | 2 |
| | $E$ | 0.4068 | 0.447 | 0.5 |
| | $R^2$ | 0.7532 | 0.7732 | 0.7854 |

equilibrium data do not follow the Freundlich isotherm model.

The constants $A_T$ and $b_T$, were obtained for the Temkin isotherm model and tabulated in Table 3. The $R^2$ value for the Temkin isotherm is 0.712 which is less than that for the Langmuir isotherm model. The constants, $q_m$ and $K$ obtained for the Dubinin–Radushkevich isotherm model were 134.42 mg/g and $2.0 \times 10^{-6}$ mol$^2$/J$^2$, respectively at 35 °C. The maximum absorption capacity, $q_m$, obtained using the D–R model was 134.42 mg/g which is less in comparison to the Langmuir model (202.34 mg/g). The mean free energy of adsorption ($E$) was obtained as 0.5 kJ/mol at 35 °C, i.e. lower than 8.0 kJ/mol. This indicates that the adsorption mechanism is governed by physical adsorption. The value of the coefficient of determination ($R^2 = 0.784$) obtained for the D–R model is significantly lower than that of the Langmuir model ($R^2 = 0.987$).

## Kinetic study

The calculated values of different kinetics parameters are presented in Table 4. The $q_e$ value can be calculated from the pseudo-first-order model (Figure 6) and pseudo-second-order model (Figure 7). The average $q_e$ values for the pseudo-first-order model were found to be 0.83, 1.57, 1.77 and 2.73 while standard deviation values were 0.78, 1.25, 1.15 and 0.90 for the concentration ranging from 100 to 250 ppm. $R^2$ values were near to 1 for all concentrations (Figure 6) which is very near to linear and comparable with experimental results. All the data follow the statistical properties and relative standard errors were found to be 46.6, 32.5, 24.5 and 12.4 for the concentration range of 100–250 ppm.

It has been found that the $q_e$ values calculated from the pseudo-second-order model are close to experimental values of $q_e$ for all Cr (VI) concentrations. The coefficient of correlation ($R^2$) was also compared for all three kinetic models and it was found that the $R^2$ value was more (near to unity) for the pseudo-second-order

**Table 4** | Kinetics parameters for adsorption of Cr (VI) on ASAC

| | Initial concentration (mg/L) | | | |
|---|---|---|---|---|
| **Kinetic parameters models** | **100** | **150** | **200** | **250** |
| $q_e$(exp) (mg/g) | 45.12 | 65.103 | 84.73 | 108.072 |
| Pseudo-first-order model | | | | |
| $k_1$ | 0.019 | 0.015 | 0.011 | 0.008 |
| $q_e$(cal) | 9.89 | 32.29 | 40.23 | 56.82 |
| $R^2$ | 0.943 | 0.991 | 0.948 | 0.962 |
| Pseudo-second-order model | | | | |
| $k_2$ | 0.1820 | 0.0546 | 0.0588 | 0.0322 |
| $q_e$(cal) | 47.6 | 71.42 | 90.90 | 125.2 |
| $R^2$ | 0.999 | 0.999 | 0.999 | 0.998 |
| Intra-particle diffusion model | | | | |
| $k_{id}$ | 0.668 | 2.281 | 3.045 | 3.460 |
| $I$ | 36.53 | 39.65 | 43.17 | 48.94 |
| $R^2$ | 0.928 | 0.965 | 0.911 | 0.939 |

model. It is seen that the intra-particle diffusion model parameters increase with increasing initial Cr (VI) concentration. The increase in the values of $I$ corresponds to the increase in boundary layer thickness which gives more importance to the surface adsorption in the rate-limiting step. Since the value of $I$ is not zero, this indicates the involvement of some other mechanisms in the adsorption process along with the intra-particle diffusion.

The average $t/q_t$ values for the second-order kinetic model were calculated as 1.75, 1.99, 1.84 and 1.54 for the concentration range of 100–250 ppm. Statistical analyses of data were carried out for the standard deviation and relative standard error to authenticate the findings and the values of RSE were found to be 24.1, 23.2, 23.0 and 21.5 corresponding to the concentrations of 100, 150, 200, and 250 ppm, respectively. These findings prove the results are statistically correct.

## Regeneration study of ASAC

Disposal of Cr (VI)-loaded activated carbon is not safe because of its environmental constraints. Hence, before disposal, it must be regenerated and the activated carbon reused. The adsorption Cr (VI) on ASAC is a physico-sorption process. In the present study, the adsorption of Cr (VI) is highly dependent on pH value and active in the lower pH range. Hence, the regeneration of Cr (VI) is achieved by increasing the solution pH through different concentrations of NaOH (1.0, 2.0 and 2.5 M). The desorption percentages for the Cr (VI) saturated adsorbents are 25.35, 54.35 and 63.45% for ASAC at the three different concentrations of NaOH. The regeneration study results indicated that a higher concentration of NaOH is effective for increasing the desorption efficiency of ASAC.

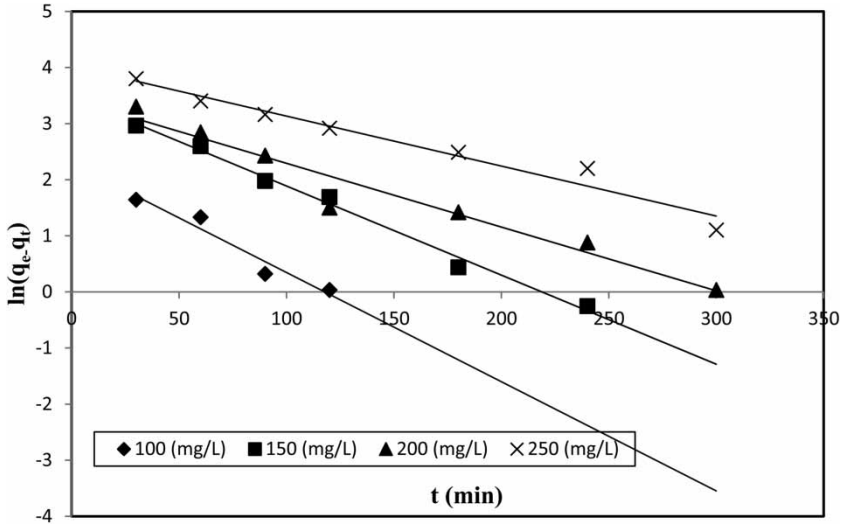


**Figure 6** | Pseudo-first-order kinetic model of Cr (VI) removal by ASAC (solution pH 2; dose 2.5 g/100 ml; agitation speed 150 rpm; temperature 35 °C).

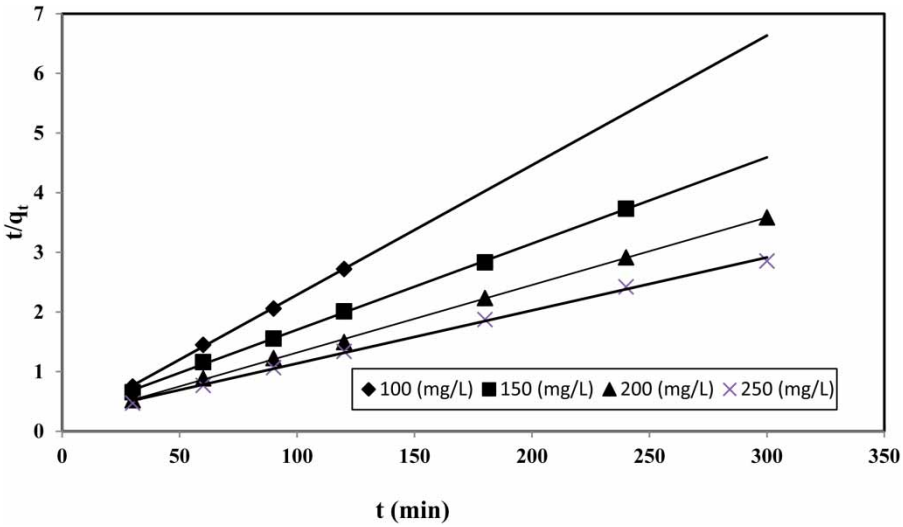


**Figure 7** | Pseudo-second-order kinetic model for Cr (VI) removal by ASAC (solution pH 2; dose 2.5 g/L; agitation speed 150 rpm; temperature 35 °C).

## Thermodynamic study

The thermodynamic parameters were obtained for initial Cr (VI) concentration of 270 mg/L at pH 2. The negative value of Gibbs free energy change indicates the feasibility and spontaneity of the adsorption process on ASAC. The enthalpy change is positive and confirms that the adsorption on ASAC was endothermic in nature. The positive value of $\Delta S$ shows that the adsorption process is governed by entropy rather than enthalpy. The values of $\Delta H^{\circ}$ and $\Delta S^{\circ}$ were found to be 22.9 KJ/mol and 95.3 J/mol-K. Rangabhashiyam & Selvaraju (2015) reported the negative $\Delta G^{\circ}$ values showed the thermodynamically feasible and spontaneous nature of the bio-sorption process for an initial Cr (VI) concentration of 100 and 200 mg/L, but the free energy change value was found to be positive at the high Cr (VI) concentrations of 300, 400 and 500 mg/L signifying the non-spontaneous nature.

## Practical application of this work

The remediation of Cr (VI) is a challenging problem due to its high level of toxicity even at very low concentration. Presence of more than the permissible level of chromium in water and soil poses severe health issues in many parts of the world. There are various techniques available for removal of chromium, each with their advantages and limitations. Cost effectiveness and affordability of the available techniques are the most important aspects. In the present study an agro-waste is utilized for conversion into biochar/activated carbon which is then used for removal of chromium with good removal efficiency. The investigated material is quite attractive because of its low cost. It will also help to reduce solid agro-waste. Another advantage of biochar is that it improves the fertility of soil. Therefore, it can be effectively used to remove the chromium toxicity of the soil along with improving its fertility.

## Future research prospects

The development process can be extended to a pilot-plant-scale investigation for the wastewater treatment system for generation of design parameters for scale-up. Further, the developed process can be employed at commercial scale in existing treatment systems with some retrofitting to the existing operation units. A few important and useful outcomes include the removal of Cr (VI) toxicity to living beings, and also the treated biochar/activated carbon may be useful in agriculture as a bio-fertilizer to enhance the soil quality by increasing the fertility. Further research in the following direction is required to establish the potential of the biochar/activated carbon developed in the present work for real-time applications: (a) the possibility of regeneration/reuse of the biochar/activated carbon should be explored;

(b) the work should be planned to use the material for reducing chromium toxicity of soil; and (c) the work should be planned using the biochar/activated carbon along with the microbial population able to convert chromium into non-toxic forms.

## CONCLUSIONS

In the present study, ASAC was prepared and used as a base material for the removal of Cr (VI). Characterization results show a very high BET surface area of 1,223.4 $m^2$/g, presence of favorable functional groups for adsorption, and a highly porous structure with greater homogeneity which makes the prepared material a perfect adsorbent. The characterization results were also validated with very high adsorption capacity of 202.34 mg/g under optimum operating conditions which shows the potential of the material for commercial application. The kinetic study of the adsorption process showed that the process followed pseudo-second-order kinetics. The thermodynamic study revealed the endothermic nature of the process.

## ACKNOWLEDGEMENTS

The authors would like to gratefully thank the DIH – Project Varanasi, IIT (BHU) for the financial support towards successful completion of this work.

## REFERENCES

Acharya, J., Sahu, J. N., Sahoo, B. K., Mohanty, C. R. & Meikap, B. C. 2009 Removal of chromium (VI) from wastewater by activated carbon developed from Tamarind wood activated with zinc chloride. *Chemical Engineering Journal* **150**, 25–39.

Anderson, L. D., Kent, D. B. & Davis, J. A. 1994 Batch experiments characterizing the reduction of chromium (VI) using sub-toxic material from a mildly reducing sand and gravel aquifer. *Environmental Science and Technology* **28**, 178–185.

Anupam, K., Dutta, S., Bhattacharjee, C. & Datta, S. 2001 Adsorptive removal of chromium (VI) from aqueous solution over powdered activated carbon: optimization through response surface methodology. *Chemical Engineering Journal* **173**, 135–143.

Baral, S. S., Das, S. N. & Rath, P. 2006 Hexavalent chromium removal from aqueous solution by adsorption on treated saw dust. *Biochemical Engineering Journal* **31**, 216–222.

Chia, C. H., Gong, B., Joseph, S. D., Marjo, C. E., Munroe, P. & Rich, A. M. 2012 Imaging of mineral-enriched biochar by FTIR, Raman and SEM-EDX. *Vibrational Spectroscopy* **62**, 248–257.

Dada, A. O., Olalekan, A. P., Olatunya, A. M. & Dada, A. O. 2012 Langmuir, Freundlich, Temkin and Dubinin–Radushkevich isotherms studies of equilibrium sorption of $Zn^{2+}$ unto phosphoric acid modified rice husk. *IOSR Journal of Applied Chemistry* **3** (1), 38–45.

Droussi, Z., Dorazio, V., Provenzano, M. R., Hafidi, M. & Ouatmane, A. 2009 Study of the biodegradation and transformation of olive-mill residues during composting using FTIR spectroscopy and differential scanning calorimetry. *Journal of Hazardous Materials* **164** (2–3), 1281–1285.

Dubinin, M. M. & Radushkevich, L. V. 1947 Equation of the characteristic curve of activated charcoal. *Chemisches Zentralblatt* **1**, 875.

Girgis, B. S., Nasser, A. A. & Hendawy, E. 2002 Porosity development in activated carbons obtained from date pits under chemical activation with phosphoric acid. *Microporous Mesoporous Materials* **52**, 105–117.

Giri, B. S., Juwarkar, A. A., Satpute, D. B., Mudliar, S. N. & Pandey, R. A. 2012 Isolation and characterization of Dimethyl Sulfide (DMS)-degrading bacteria from soil and biofilter treating waste gas containing DMS from the laboratory and pulp and paper industry. *Applied Biochemistry and Biotechnology* **167** (6), 1744–1752.

Gupta, S. & Babu, B. V. 2009 Utilization of waste product (tamarind seeds) for the removal of Cr (VI) from aqueous solutions: equilibrium, kinetics, and regeneration studies. *Journal of Environmental Management* **90**, 3013–3022.

Han, X., Wong, Y. S., Wong, M. H. & Tam, N. F. Y. 2007 Biosorption and bio-reduction of Cr (VI) by a micro algal isolate *Chlorella miniata*. *Journal of Hazardous Materials* **146**, 65–72.

Hsu, N. H., Wang, S. L., Liao, Y. H., Huang, S. T., Tzou, Y. M. & Huang, Y. M. 2009 Removal of hexavalent chromium from acidic aqueous solutions using rice straw-derived carbon. *Journal of Hazardous Materials* **171**, 1066–1070.

Imai, A. & Gloyna, E. F. 1990 Effects of pH and oxidation state of chromium on the behavior of chromium in the activated sludge process. *Water Research* **24**, 1143–1150.

Kanjanarong, J., Giri, B. S., Jaisi, D. P., Oliveira, F. R., Boonsawang, P. & Khanal, S. K. 2017 Removal of hydrogen sulfide generated during anaerobic treatment of sulfate-laden waste water using biochar: evaluation of efficiency and mechanisms. *Bioresource Technology* **234**, 115–121.

Karacetin, G., Sivrikaya, S. & Imamoglu, M. 2014 Adsorption of methylene blue from aqueous solutions by activated carbon prepared from hazelnut husk using zinc chloride. *Journal of Analytical and Applied Pyrolysis* **110**, 270–276.

Karthikeyan, T., Rajgopal, S. & Miranda, L. R. 2005 Chromium (VI) adsorption from aqueous solution by *Hevea brasilinesis* saw dust activated carbon. *Journal of Hazardous Materials* **124** (1–3), 192–199.

Kumar, J. A. & Mandal, B. 2009 Removal of Cr (VI) from aqueous solution using Bael fruit (*Aegle marmeloscorrea*) shell as an adsorbent. *Journal of Hazardous Materials* **168**, 633–640.

Langmuir, I. 1918 The adsorption of gases on plane surfaces of glass, mica and platinum. *Journal of American Chemical Society* **40**, 1361–1403.

Mohan, D., Singh, K. P. & Singh, V. K. 2005 Removal of hexavalent chromium from aqueous solution using low-cost activated carbons derived from agricultural waste materials and activated carbon fabric cloth. *Industrial and Engineering Chemistry Research* **44**, 1027–1042.

Mohan, D., Singh, K. P. & Singh, V. K. 2006 Trivalent chromium removal from wastewater using low cost activated carbon derived from agricultural waste material and activated carbon fabric cloth. *Journal of Hazardous Materials* **135** (1–3), 280–295.

Mohanty, K., Jha, M., Meikap, B. C. & Biswas, M. N. 2005 Removal of chromium (VI) from dilute aqueous solutions by activated carbon developed from *Terminalia arjuna* nuts activated with zinc chloride. *Chemical Engineering Science* **60**, 3049–3059.

Nakajima, A. & Baba, Y. 2004 Mechanism of hexavalent chromium adsorption by persimmon tannin gel. *Water Research* **38**, 2859–2864.

Nemr, A. E. 2009 Potential of pomegranate husk carbon for Cr (VI) removal from wastewater: kinetic and isotherm studies. *Journal of Hazardous Materials* **161**, 132–141.

Onal, Y., Basar, A. C., Ozdemir, S. C. & Erdogan, S. 2007 Textural development of sugar beet bagasse activated with $ZnCl_2$. *Journal of Hazardous Materials* **142**, 138–143.

Othman, Z. A. A., Ali, R. & Naushad, M. 2012 Hexavalent chromium removal from aqueous medium by activated carbon prepared from peanut shell: adsorption kinetics, equilibrium and thermodynamic studies. *Chemical Engineering Journal* **184**, 238–247.

Owlad, M., Aroua, M. K., Daud, W. A. W. & Baroutian, S. 2009 Removal of hexavalent chromium-contaminated water and wastewater: a review. *Water Air Soil Pollution* **200**, 59–77.

Ozdemir, E., Duranoglu, D., Beker, U. & Avci, A. O. 2011 Process optimization for Cr (VI) adsorption onto activated carbons by experimental design. *Chemical Engineering Journal* **172** (1), 207–218.

Park, D., Lim, S. R., Yun, Y. S. & Park, J. M. 2007 Reliable evidences that the removal mechanism of hexavalent chromium by natural biomaterials is adsorption-coupled reduction. *Chemosphere* **70**, 298–305.

Pedroza, M. M., Sousa, J. F., Vieira, G. E. G. & Bezerra, M. B. D. 2014 Characterization of the products from the pyrolysis of sewage sludge in 1 kg/h rotating cylinder reactor. *Journal of Analytical and Applied Pyrolysis* **105**, 108–115.

Rai, M. K., Shahi, G., Meena, V., Meena, R., Chakraborty, S., Singh, R. S. & Rai, B. N. 2016 Removal of hexavalent chromium Cr (VI) using activated carbon prepared from mango kernel activated with $H_3PO_4$. *Resource Efficient Technology* **2**, 63–70.

Rangabhashiyam, S. & Selvaraju, N. 2015 Adsorptive remediation of hexavalent chromium from synthetic wastewater by a natural and $ZnCl_2$ activated *Sterculia guttata* shell. *Journal of Molecular Liquids* **207**, 39–49.

Selvi, K., Pattabhi, S. & Kadirvelu, K. 2001 Removal of Cr (VI) from aqueous solution by adsorption onto activated carbon. *Bioresource Technology* **80**, 87–89.

Singh, K., Giri, B. S., Sahi, A., Geed, S. R., Kureel, M. K., Singh, S., Dubey, S. K., Rai, B. N., Kumar, S., Upadhyay, S. N. & Singh, R. S. 2017 Biofiltration of xylene using wood charcoal as the biofilter media under transient and high loading conditions. *Bioresource Technology* **242**, 351–358.

Sonwani, R., Giri, B. S., Sharma, A., Singh, R. S. & Rai, B. N. 2018 Combination of UV-Fenton oxidation process with biological technique for treatment of polycyclic aromatic hydrocarbons using Pseudomonas pseudoalcaligenes NRSS3 isolated from petroleum contaminated site. *Indian Journal of Experimental Biology (IJEB)* **56** (7), 460–469.

Stasinakis, A. S., Thomaidis, N. S., Mamais, D., Karivali, M. & Lekkas, T. D. 2003 Chromium species behavior in the activated sludge process. *Chemosphere* **52**, 1059–1067.

Suksabye, P. & Thiravetyan, P. 2012 Cr (VI) adsorption from electroplating plating wastewater by chemically modified coir pith. *Journal of Environment Management* **102**, 1–8.

Talha, M. A., Goswami, M., Giri, B. S., Sharma, A., Rai, B. N. & Singh, R. S. 2018 Bioremediation of Congo red dye in immobilized batch and continuous packed bed bioreactor by *Brevibacillus parabrevis* using coconut shell bio-char. *Bioresource Technology* **252**, 37–43.

Tan, C., Zeyu, Z., Sai, X., Hongtao, W. & Wenjing, L. 2015 Adsorption behaviour comparison of trivalent and hexavalent chromium on biochar derived from municipal sludge. *Bioresource Technology* **190**, 388–394.

Tempkin, M. J. & Pyzhev, V. 1940 Kinetics of ammonia synthesis on promoted iron catalysts. *Acta Physicochimica URSS* **12**, 217–222.

Ugurlu, M. & Karaoglu, H. 2008 Adsorption of Cd (II) ions from aqueous solutions using activated carbon prepared from olive stone by $ZnCl_2$ activation. *Bioresource Technology* **99**, 492–501.

Verma, A., Chakraborty, S. & Basu, J. K. 2006 Adsorption study of hexavalent chromium using tamarind hull-based adsorbents. *Separation and Purification Technology* **50**, 336–341.

Wang, S. Y., Tang, Y. K., Li, K., Mo, Y. Y., Li, H. F. & Gu, Z. Q. 2014 Combined performance of biochar sorption and magnetic separation processes for treatment of chromium-contained electroplating wastewater. *Bioresource Technology* **174**, 67–73.

Weber, W. J. & Morris, J. C. 1962 Advances in water pollution research: removal of biologically resistant pollutants from waste waters by adsorption. In: *Proceedings of International*

*Conference on Water Pollution Symposium*. Pergamon Press, Oxford, 2, pp. 231–266.

Yang, J. & Chen, M. Y. W. 2015 Adsorption of hexavalent chromium from aqueous solution by activated carbon prepared from Longan seed: kinetics, equilibrium and thermodynamics. *Journal of Industrial and Engineering Chemistry* **21**, 414–422.

Zhang, B., Xiong, S., Xiao, B., Yu, D. & Jia, X. 2011 Mechanism of wet sewage sludge pyrolysis in a tubular furnace. *International Journal of Hydrogen Energy* **36** (1), 355–363.

First received 20 April 2018; accepted in revised form 2 August 2018. Available online 27 August 2018